Series of phase transitions in cesium azide under high pressure studied by *in situ* x-ray diffraction

Dongbin Hou,[1] Fuxiang Zhang,[2] Cheng Ji,[1] Trevor Hannon,[1] Hongyang Zhu,[1] Jianzhe Wu,[1] and Yanzhang Ma[1,*]

[1] *Department of Mechanical Engineering, Texas Tech University, Lubbock, Texas 79409, USA*

[2] *Department of Geological Sciences, University of Michigan, Ann Arbor, Michigan 48109-1005, USA*

(Received 31 January 2011; revised manuscript received 29 March 2011; published 30 August 2011)

In situ x-ray diffraction measurements of cesium azide (CsN_3) were performed at high pressures of up to 55.4 GPa at room temperature. Three phase transitions were revealed as follows: tetragonal ($I4/mcm$, Phase II) → monoclinic ($C2/m$, Phase III) → monoclinic ($P2_1/m$ or $P2_1$, Phase IV) → triclinic ($P1$ or $P\bar{1}$, Phase V), at 0.5, 4.4, and 15.4 GPa, respectively. During the II–III phase transition, CsN_3 keeps its layered structure and the azide anions rotate obviously. The compressibility of Phase II is dominated by the repulsions between azide anions. The deformation of unit cell is isotropic in Phases II and IV and anisotropic in Phase III. With increasing pressures, the monoclinic angle increases in Phase III and then becomes stable in Phase IV. The bulk moduli of Phases II, III, IV, and V are determined to be 18 ± 4, 20 ± 1, 27 ± 1 and 34 ± 1 GPa, respectively. The ionic character of alkali azides is found to play a key role in their pressure-induced phase transitions.

DOI: 10.1103/PhysRevB.84.064127 PACS number(s): 81.40.Vw, 61.50.Ks, 61.66.Fn, 62.20.−x

I. INTRODUCTION

Inorganic azides are important materials[1–3] because of their practical and their theoretical applications. Practically, they are widely applied as explosives and pure nitrogen gas sources[4–6]; theoretically, they are simple systems that can be used in modeling the interatomic forces to study both the structure and the dynamics in various phases under different conditions.[7–9]

Alkali azides, a comparably stable species among inorganic azides, exhibit a variety of phase transitions stimulated by either temperature or pressure.[9–20] During these transitions, the behavior of the azide anions N_3^- is noticeable. In the temperature-induced phase transitions of both rubidium azide (RbN_3) and cesium azide (CsN_3), a fluctuation of the orientation of N_3^- anions was shown.[11–13] In both the pressure-[10] and the temperature-induced[18–20] phase transitions of sodium azide (NaN_3), a tilting of N_3^- anions was also exhibited. Recently, the high-pressure effect on alkali azides has become a promising topic because of azides' application as precursors to synthesize a high energetic density material of a polymeric (nonmolecular) form of nitrogen (N_2). A polymeric nitrogen phase under high pressure was first predicted in 1985.[21] It was investigated with optical and electrical methods in 2000[22] and 2001,[23] respectively. A single-bonded cubic gauche form of N_2 was successfully synthesized in 2004[24] and 2007.[25] The N_3^- anions of NaN_3 at high pressure were observed to transform to polymeric nitrogen nets in 2004[14] and a cubic gauche structure in 2005.[15] The formation of a polymeric nitrogen network was also predicted on lithium azide (LiN_3) under high pressure.[26] The mechanism of photolysis of NaN_3 under high pressure was also investigated to elucidate the potential to synthesize the high energetic density nitrogen structures.[27] In this respect, an investigation of the high-pressure behavior of CsN_3 would provide more insight into the pressure-induced rearrangement of N_3^- anions and phase transitions that might form the high energetic density material of polymeric nitrogen.

Under ambient conditions, CsN_3 crystallizes in a body-centered tetragonal system with space group $I4/mcm$ and lattice parameters $a = 6.5412$ Å and $c = 8.0908$ Å (Phase II).[28] This particular tetragonal structure can be understood as a distorted cesium–chloride cubic structure ($Pm3m$) caused by the asphericity of the linear N_3^- anions (Fig. 1). At 151 °C and ambient pressure, CsN_3 undergoes a phase transition from the tetragonal Phase II to a cubic form in space group $Pm3m$ (Phase I).[11] In contrast of Phase II, Phase I has randomly orientated N_3^- anions with respect to the edges of the cubic unit cell.[11–13] Around 0.4 GPa and 25.7 °C, Phase II transforms to a high-pressure form (Phase III) with a volume reduction of 4.2%.[9] A Raman study suggests that Phase III involves at least two crystallographically nonequivalent N_3^- ion sites,[12] but the crystal structure of Phase III has not yet been determined.

The present paper reports the high-pressure phases and the compressibility of CsN_3 by means of a synchrotron x-ray diffraction measurement to 55.4 GPa in a diamond anvil cell.

II. EXPERIMENTAL

A symmetric diamond anvil cell with flat diamonds was used to generate high pressure in the experiments. The anvil was 400 μm in diameter. A rhenium gasket was used, with a hole 150 μm in diameter and 60 μm in thickness, as a sample chamber. The 99.99% CsN_3 powder was obtained from Sigma Aldrich (USA). A small flake of the sample with an ~100 μm diameter and ~30 μm thickness was loaded into the sample chamber. Pressure was measured by the nonlinear shift of the wavelength of the ruby R1 line.[29,30] Neon gas, mineral oil, and silicone oil were selected as pressure transmitting media in different experimental runs to rule out the possible contamination by products of the reaction of CsN_3 with the pressure media. *In situ* high-pressure angle-dispersive x-ray diffraction experiments at room temperature were performed at the beamline B2 of the Cornell High Energy Synchrotron Source (CHESS, Wilson Laboratory) at Cornell University and the beamline X17C in the National Synchrotron Light Source (NSLS) at Brookhaven National Laboratory. The experiments using mineral oil and neon as pressure media were performed in CHESS, and those using silicone oil were performed in

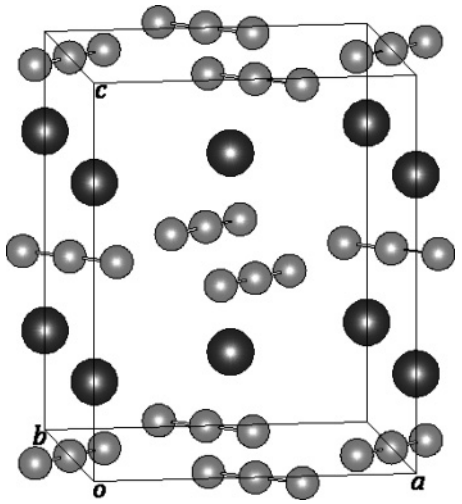

FIG. 1. The crystal structure of Phase II. The Cs atoms are represented by black spheres and the N atoms by gray spheres.

NSLS. In the NSLS experiments, the sample was ground for a longer time than in the CHESS experiments to obtain more randomly oriented microcrystals of the sample. In CHESS, the x-ray had a wavelength of 0.4859 Å and was collimated to a beam size that was 40 μm in diameter; the diffraction data were recorded on a MAR345 imaging plate. In NSLS, the x-ray beam had a wavelength of 0.4066 Å and was focused to a spot size of 27×21 μm^2; the diffraction data were collected using a Mar charge-coupled device (CCD) detector. The diffraction images were converted to 2θ versus intensity data plots using FIT2D software.[31]

III. RESULTS AND DISCUSSION

The results revealed three pressure-induced phase transitions (II–III, III–IV, and IV–V) up to 55.4 GPa. For the first one, because Phase II was observed at 0.4 GPa and Phase III was observed at 0.5 GPa, the onset of the II–III transition lies between 0.4 and 0.5 GPa. It is in excellent agreement with the II–III boundary reported by Pistorius at 0.409 ± 0.042 GPa,[9] given the 0.1 GPa uncertainty in the ruby florescence pressure measurement system.[32] The second transition (III–IV) was observed by a coexistence of Phases III and IV at 4.4 GPa. And because only Phase III was observed at 3.8 GPa and only Phase IV was observed at 5.0 GPa, it can be inferred that the onset of the III–IV transition lies between 3.8 and 4.4 GPa and the completion lies between 4.4 and 5.0 GPa. The third transition (IV–V) is considerably sluggish. The coexistence of Phases IV and V was observed over the pressure range from 15.4 to 23.7 GPa. The onset of the IV–V transition lies between 15.1 and 15.4 GPa, and the completion lies between 23.7 and 24.7 GPa. Phase V is stable up to the highest pressure attained (55.4 GPa). During the decompression process, Phase V was retained at 8.6 GPa, Phases IV and V coexisted at 3.5 GPa, and Phase II was recovered when pressure was released back to ambient conditions. The phase transition pressures are summarized in Table I, and the representative diffraction patterns are shown in Fig. 2(a).

The Bragg peak positions were determined by the program Peakfit v4.11 (Systat Software). At ambient conditions, 12 peaks were resolved and indexed to the tetragonal structure with $I4/mcm$ symmetry (Phase II). The cell parameters obtained at ambient conditions, $a = b = 6.545 \pm 0.001$ and $c = 8.103 \pm 0.002$, are in excellent agreement with the results in the literature.[28] In the investigation of the unknown structure of each high-pressure phase, the crystal system and unit cell were yielded by indexing the Bragg peaks using the program Dicvol04,[33] the number of formula units per unit cell (the Z number) was calculated from volume decrements, and the space group was determined by the systematic extinctions listed in the international tables for crystallography (Volume A).[34]

TABLE I. Phase transition pressures of CsN_3.

	II–III	III–IV	IV–V
P_i (GPa)[a]	$0.4 \sim 0.5$	$3.8 \sim 4.4$	$15.1 \sim 15.4$
P_c (GPa)[b]	$0.4 \sim 0.5$	$4.4 \sim 5.0$	$23.7 \sim 24.7$

[a] P_i indicates the initial pressure of phase transition.
[b] P_c indicates the completion pressure.

For Phase III, indexing using Dicvol04 yielded a unique solution, which led to a unit cell in monoclinic symmetry with $Z = 4$. In its diffraction pattern, a systematic extinction of (hkl) with $h + k$ odd was observed, so the possible space groups of Phase III are $C2$, Cm, and $C2/m$. Because the ambient CsN_3 (tetragonal Phase II) belongs to the point group of $4/mmm$, its high-pressure form (monoclinic Phase III) is more probable in the point group of $2/m$ than 2 or m (the degrade of symmetry element from the four- to twofold axis and the loss of mirror planes can be ascribed to the distortion of the unit cell from tetragonal to monoclinic). Moreover, among all known structures of alkali azides (including the phases at nonambient conditions), there exist two monoclinic structures (LiN_3 and α-NaN_3), both of which belong to the $C2/m$ space group.[10] Therefore, the space group of CsN_3 Phase III was assigned as $C2/m$.

For Phase IV, the crystal system was determined to be monoclinic, because all indexing solutions led to the monoclinic symmetry. The most probable index yielded a unit cell with $Z = 8$. A systematic extinction was observed, $(0k0)$ with k odd; therefore, the space group of Phase IV was determined to be $P2_1/m$ or $P2_1$ (both have the same systematic extinction due to symmetry).

For Phase V, the crystal system was determined to be triclinic, because all indexing solutions led to a triclinic symmetry. The most probable index yielded a unit cell with

TABLE II. Atomic fractional coordinates of Phase III at 2.9 GPa.

Atom	Wyck[a]	x[b]	y	z[b]
Cs	$4i$	−0.0196(7)	0	0.2745(5)
N_1	$2b$	0	0.5	0
N_2	$2d$	0	0.5	0.5
N_3	$4i$	0.1716(9)	0.5	0.4914(6)
N_4	$4i$	0.1716(9)	0.5	−0.0086(6)

[a] Wyck stands for the Wyckoff positions of space group $C2/m$.
[b] The number in parentheses represents the error in the last digit resulting from the refinement.

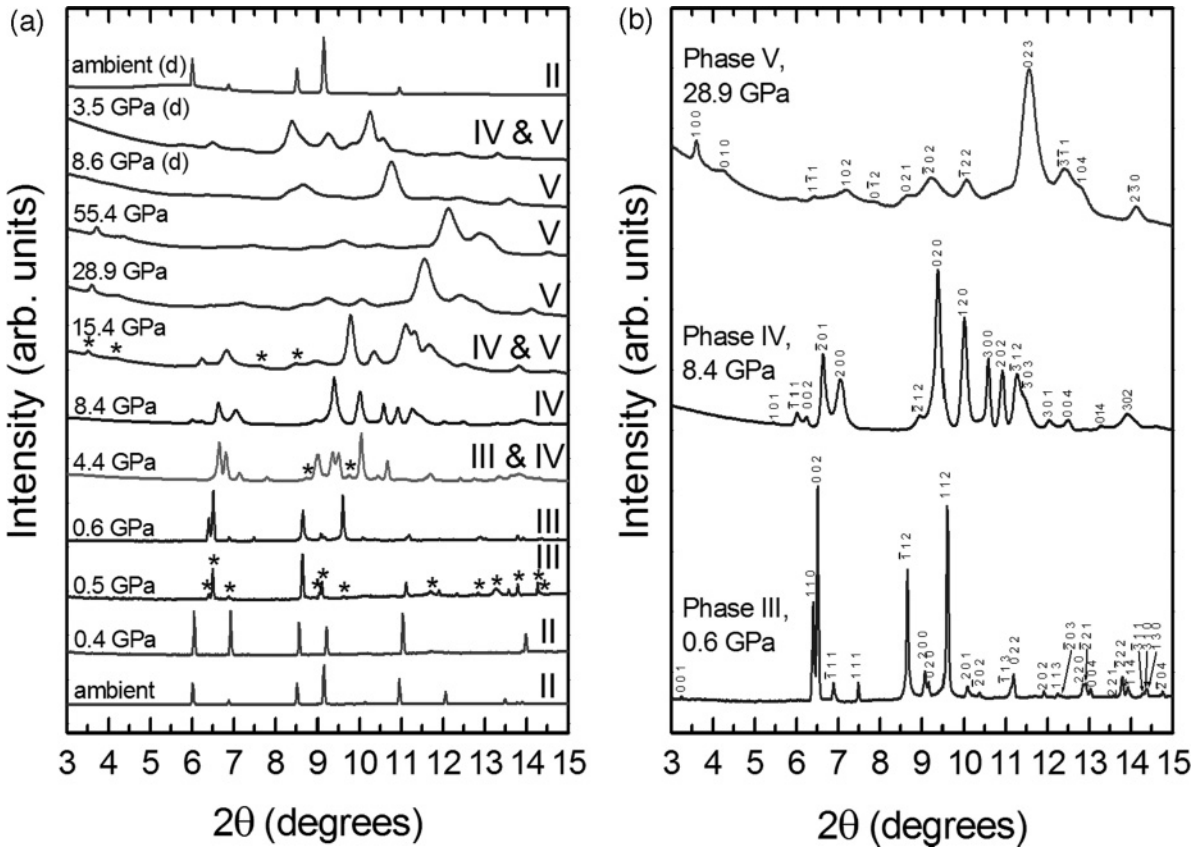

FIG. 2. X-raydiffraction patterns of CsN_3 at selected pressures. (a) Different phases, shown by the Roman numerals to the right of the patterns. The coexistence of two phases at 4.4 and 15.4 GPa indicates the onset of the phase transitions. The asterisks indicate the appearance of new Bragg peaks due to the phase transitions. The three patterns on the top of the figure (with a letter "d" in parentheses besides the pressure) demonstrate the decompression process. (b) The Miller indices of the high-pressure phases.

$Z = 12$. The space group of Phase V was determined to be $P1$ or $P\bar{1}$, because these are the only possible space groups in triclinic symmetry and neither of them has a systematic extinction. The indexing of Phases III, IV, and V are shown in Fig. 2(b).

To investigate the atomic fractional coordinates of Phase III, the diffraction pattern obtained at 2.9 GPa in NSLS was refined using Rietveld method with FullProf software.[35] To construct the original structure for the refinement, an investigation of all known structures of alkali azides was performed, and it was found all of them have linear azide anions, with either parallel or perpendicular arrangements to one another[10,36] (which can be understood because the parallel or perpendicular arrangement is energetically favorable). Moreover, it was also observed that in all structures with an orthogonal unit cell ($a \perp b \perp c$), the azide chains are perpendicular to one another (as seen in KN_3, α-RbN_3, and CsN_3, or Phase II[36]) and that in all structures with an nonorthogonal unit cell, the azide chains are parallel (as seen in LiN_3, α-NaN_3, and β-NaN_3[10,36]). Because CsN_3 Phase III has a nonorthogonal unit cell, a parallel chain structure for the azide anions was applied in the refinement. Because the II–III phase transformation happens at a relative low pressure (0.5 GPa), it is reasonable to assume the atoms in Phase III reside on positions similar to those of Phase II. Therefore, the Wyckoff positions of Cs and four N atoms were

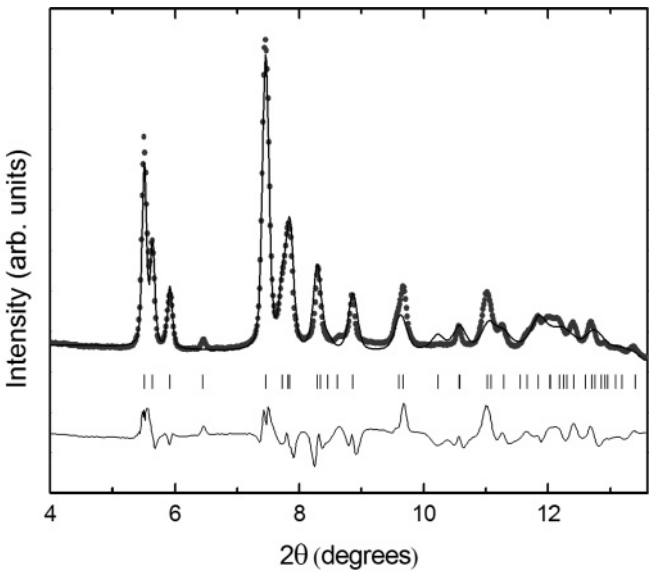

FIG. 3. Rietveld refinement patterns for Phase III at 2.9 GPa. The observed diffraction intensities are represented by the dots, and the calculated pattern is represented by the solid line. The solid curve at the bottom represents the difference between the observed and the calculated intensities. Short vertical bars below the observed and the calculated patterns indicate the positions of allowed Bragg reflections.

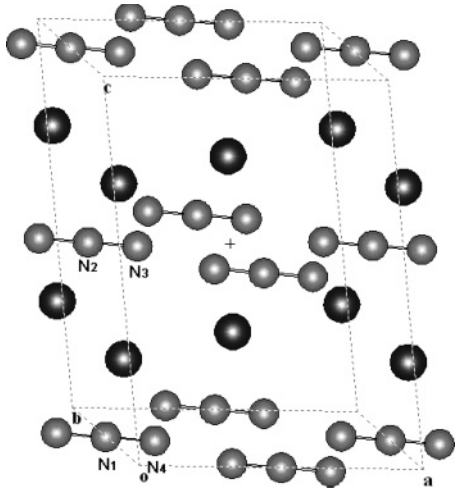

FIG. 4. The crystal structure of Phase III yielded from the refinement at 2.9 GPa. The Cs atoms are represented by black spheres and the N atoms by gray spheres.

assigned to be *4i*, *2b*, *2d*, *4i*, and *4i*, respectively (as seen in Table II). The mean quality factors of the refinement are $R_p = 6.19\%$, $R_{wp} = 8.24\%$, and $\chi^2 = 1.47$, and the Rietveld plot is shown in Fig. 3. The resulted atomic fractional coordinates are summarized in Table II and plotted in Fig. 4. The results indicate that the azide anion chains N_4-N_1-N_4 and N_3-N_2-N_3 reside on two crystallographically nonequivalent sites, which is in agreement with the results from the previous Raman study.[12] The results show that CsN_3 keeps its layered structure and the orientation of azide anions rotates obviously during the II–III transition. Unlike those lying in the *ab* plane in Phase II, the azide anions tilt up slightly at an angle of 3.85° in Phase III. The tilt of azide anions may be ascribed to the shear of layers, a phenomenon also seen in LiN_3[26] and NaN_3.[10] The atomic fractional coordinates of Cs deviate slightly from their values in Phase II. In Phase II, the Cs atom resides on the special Wyckoff position *4a* at (0, 0, 0.25), whereas in Phase III, it resides on the general Wyckoff position *4i* at (-0.0196 ± 0.0007, 0, 0.2745 ± 0.0005). The sum of the ionic radii of Cs and N is 3.32 Å[28] under ambient conditions. If we assume the shrink of ionic radii is proportional to the shrink of the unit cell volume, the sum of ionic radii of Cs and N will become 2.88 Å at 2.9 GPa, which is 8% bigger than the shortest distance between Cs and N yielded in the refinement (2.67 Å). Thus, we do not exclude the possibility that cesium forms some degree of covalent bonding with the azide group under high pressure. The atomic fractional coordinates of N_3 and N_4 that resulted from the fitting may not be accurate because of the large difference in the scattering ability of Cs and N and because of the nonperfect fitting (as shown in Fig. 3, the difference between the observed and the calculated patterns) due to the preferred orientation in the sample; nevertheless, the trend of change during the phase transition should be reliable.

To reveal the compressibility of each phase, the cell parameters and volume per formula unit were computed from the peak positions measured at varying pressures.[37] The changes of cell parameters are illustrated in Figs. 5 and 6. For Phase II, the compressibility of the *c* direction has little difference from that of the *a* direction when we take into account the experimental errors [Fig. 5(b)], which contrasts with the observation that the Cs-Cs distances in the *c* direction are much shorter than those in the [1 1 0] directions (4.045 for Cs-Cs distance and 4.625 Å in [1 1 0] direction, respectively, in Phase II under ambient conditions[28]). This implies that the repulsions between azide anions dominate the compressibility behavior of Phase II.

For Phase III, the smallest deformation occurs along the *a* axis, and the deformations along the *b* and *c* axes are equivalent [Fig. 5(c)]. The monoclinic angle β of Phase III increases under compression (a linear fitting of the Pressure-β data of Phase III yields a slope of $0.16 \pm 0.02°$ GPa^{-1}, as shown in Fig. 6). This interlayer shear may imply a tilt of the azide anions during the compression, a phenomenon that was also observed in the high-pressure behavior of LiN_3.[26]

For Phase IV, compressibility shows isotropy in all three directions, *a*, *b*, and *c* [Fig. 5(d)], and the monoclinic angle β shows little change with increasing pressure (a linear fitting of the P-β data of Phase IV yields a slope of $0.012 \pm 0.009°$ GPa^{-1}, as shown in Fig. 6). The isotropic compressibility and stable monoclinic angle of Phase IV infer that its unit cell keeps the same geometric shape and shrinks uniformly under compression. This may imply that the atomic fractional

TABLE III. Comparison of properties and phase transition pressures of alkali azides.

Alkali azides	Δ(N-N)	Metal-end N bond order	Phase transition pressures (under room temperature)
LiN_3	0.006[a]	0.14[a]	No transitions $\geqslant$ 62 GPa[b]
α-NaN_3	0.005[a]	0.12[a]	19 GPa[c]
KN_3	0.003[a]	0.02[a]	15.5 GPa[d]
α-RbN_3	0.002[a]	0[a]	0.5 GPa[e]
CsN_3 (Phase II)	0.001[a]	0[a]	0.4 GPa,[e] 0.4∼0.5 GPa[f]

[a]Reference 36.
[b]Reference 26.
[c]Reference 14.
[d]Reference 39.
[e]Reference 9.
[f]This study.

coordinates of Phase IV have little change with increasing pressure, which infers that the azide anions of Phase IV keep almost the same orientation during compression.

Figure 7 shows the volume per formula unit as a function of pressure. The volume reduction of the II–III transition is 4% from 0.4 to 0.5 GPa in this study, which is in agreement with the study of Pistorius.[9] By fitting the Phase V data of each phase to the second-order Birch-Murnaghan equation of state,[38] the bulk moduli of Phases II, III, IV, and V were yielded as 18 ± 4, 20 ± 1, 27 ± 1, and 34 ± 1 GPa, respectively. The increasing bulk moduli infer an enhancement of bond strength during phase transitions.

A comparison of the properties and phase transition pressures of alkali azides are given in Table III to provide insight into the phase transition mechanism. A previous theoretical work reported that the closeness of the internitrogen distances of the alkali azides to the calculated N-N bond length for the free azide ion Δ(N-N) has the following order for the alkali azides: $LiN_3 > \alpha$-$NaN_3 > KN_3 > \alpha$-$RbN_3 > CsN_3$ (Phase II).[36] Moreover, the bond order for the alkali metal-end N bonds decreases in the same order.[36] (The bond order is a measure of the overall bond strength between two atoms. A high value of the bond order indicates a stronger bond with a covalent character, whereas a low value shows a weaker bond with an ionic nature.[36]) These two facts indicate that their ionic character intensifies in the following sequence: $LiN_3 < \alpha$-$NaN_3 < KN_3 < \alpha$-$RbN_3 < CsN_3$ (Phase II).[36] However, the transition pressures of the alkali azides decrease in the order of $LiN_3 > \alpha$-$NaN_3 > KN_3 > \alpha$-$RbN_3 > CsN_3$ (Phase II).[9,14,26,39] Therefore, it can be concluded that the ionic character of the compounds plays a key role in the pressure-induced phase transitions of alkali azides (more specifically,

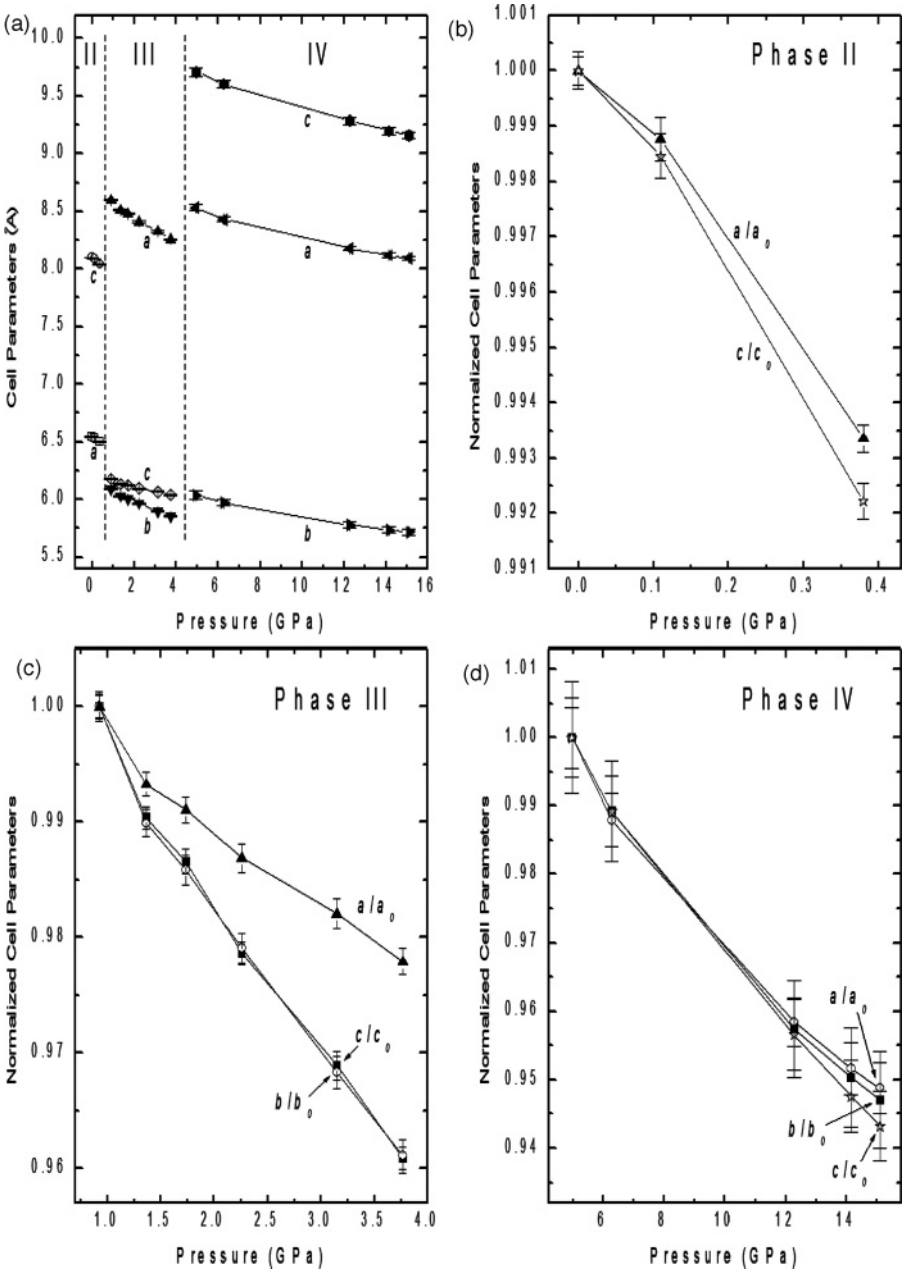

FIG. 5. The pressure dependence of the cell parameters a, b, and c of CsN_3.

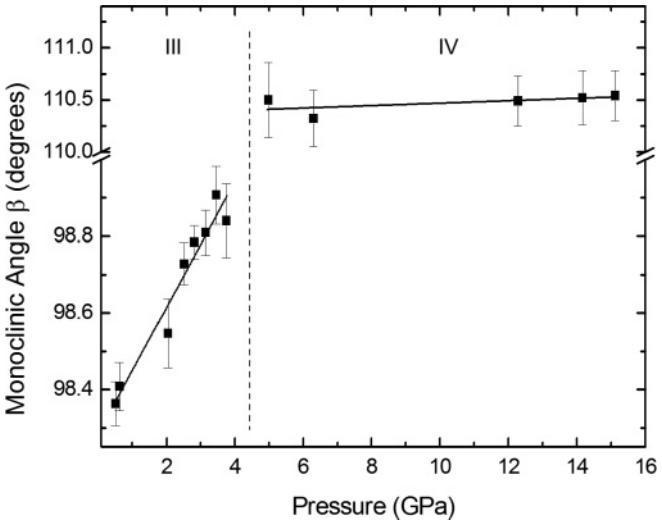

FIG. 6. The pressure dependence of the monoclinic angle β of Phases III and IV. The solid lines demonstrate the linear fitting of the P-β data.

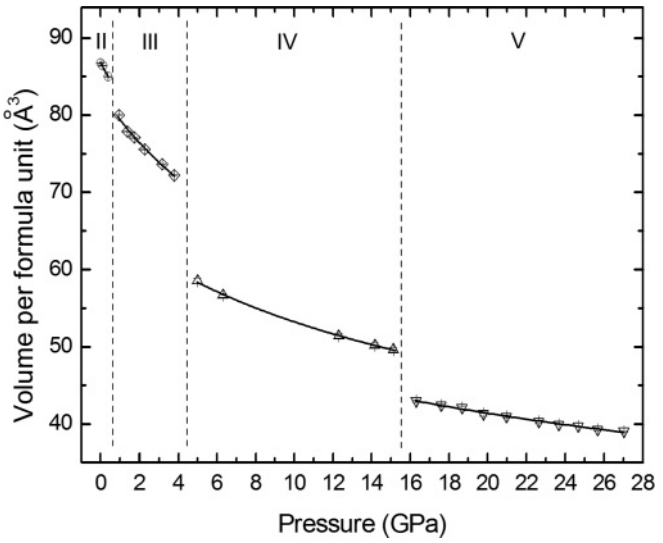

FIG. 7. Volume per formula unit change of CsN_3 with pressure. The solid lines demonstrate the fitting of the Phase V data to the second-order Birch-Murnaghan equation of state.

the phase transitions are favored by a stronger ionic character of the compounds). This can be understood because in the alkali azides, all available valencies are bound to azide groups; thus, their phase stability is dominated by their ionic character.

IV. SUMMARY AND CONCLUSIONS

A high-pressure study of CsN_3 up to 55.4 GPa revealed three phase transitions at 0.5, 4.4, and 15.4 GPa. The space groups for the high-pressure phases were determined to be as follows: Phase III is $C2/m$, Phase IV is $P2_1/m$ or $P2_1$, and Phase V is $P1$ or $P\bar{1}$. During the II–III transition, the layered structure is retained and the azide anions rotate obviously. The compressibility of cell parameters a, b, and c is isotropic in Phases II and IV but anisotropic in Phase III. The monoclinic angle β of Phase III increases under compression, whereas the β angle of Phase IV shows little change with increasing pressure. The bulk moduli of Phases II, III, IV, and V are determined to be 18 ± 4, 20 ± 1, 27 ± 1, and 34 ± 1 GPa, respectively. The ionic character of alkali azides plays a key role in their pressure-induced phase transitions.

ACKNOWLEDGMENTS

Thanks are due to Z. Wang for his technical assistance. This work was supported by the Defense Threat Reduction Agency (HDTRA1-09-0034), the Army Research Office (W911NF-09-1-0001), and the National Science Foundation (DMR-0619215).

*Corresponding author: y.ma@ttu.edu

[1] B. L. Evans and A. D. Yoffe, Proc. R. Soc. London A **238**, 568 (1957).
[2] B. L. Evans, A. D. Yoffe, and P. Gray, Chem. Rev. (Washington, DC) **59**, 515 (1959).
[3] I. Agrell, Acta Chem. Scand. **25**, 2965 (1971).
[4] C. M. Pereira and M. M. Chaudhri, J. Energ. Mater. **7**, 297 (1989).
[5] B. P. Aduev, E. D. Aluker, G. M. Belokurov, Y. A. Zakharov, and A. G. Krechetov, J. Exp. Theor. Phys. **89**, 906 (1999).
[6] S. K. Deb, B. L. Evans, and A. D. Yoffe, Symp. (Int.) Combust. [Proc.] **8**, 829 (1962).
[7] C. E. Weir, S. Block, and G. J. Piermarini, J. Chem. Phys. **53**, 4265 (1970).
[8] J. Liu, C. G. Duan, M. M. Ossowski, W. N. Mei, R. W. Smith, and J. R. Hardy, Mater. Res. Bull. **36**, 2035 (2001).
[9] C. W. F. T. Pistorius, J. Chem. Phys. **51**, 2604 (1969).
[10] G. E. Pringle and D. E. Noakes, Acta Crystallogr. B **24**, 262 (1968).
[11] H. J. Mueller and J. A. Joebstl, Z. Kristallogr. Kristallgeom. Kristallphys. Kristallchem. **121**, 385 (1965).
[12] Z. Iqbal and C. W. Christoe, J. Chem. Phys. **62**, 3246 (1975).
[13] F. J. Owens, J. Phys. C **12**, 2255 (1979).
[14] M. I. Eremets, M. Y. Popov, I. A. Trojan, V. N. Denisov, R. Boehler, and R. J. Hemley, J. Chem. Phys. **120**, 10618 (2004).
[15] M. Popov, Phys. Lett. A **334**, 317 (2005).
[16] Z. Iqbal and C. W. Christoe, Solid State Commun. **17**, 71 (1975).
[17] S. R. Aghdaee and A. I. M. Rae, Acta Crystallogr. B: Struct. Sci. **B40**, 214 (1984).
[18] G. J. Simonis and C. E. Hathaway, Phys. Rev. B **10**, 4419 (1974).
[19] L. B. Kanney, N. S. Gillis, and J. C. Raich, J. Chem. Phys. **67**, 81 (1977).
[20] Z. Iqbal, J. Chem. Phys. **59**, 1769 (1973).
[21] A. K. McMahan and R. LeSar, Phys. Rev. Lett. **54**, 1929 (1985).
[22] A. F. Goncharov, E. Gregoryanz, H.-K. Mao, Z. Liu, and R. J. Hemley, Phys. Rev. Lett. **85**, 1262 (2000).

[23]M. I. Eremets, R. J. Hemley, H.-K. Mao, and E. Gregoryanz, Nature (London) **411**, 170 (2001).
[24]M. I. Eremets, A. G. Gavriliuk, I. A. Trojan, D. A. Dzivenko, and R. Boehler, Nat. Mater. **3**, 558 (2004).
[25]M. I. Eremets, A. G. Gavriliuk, and I. A. Trojan, Appl. Phys. Lett. **90**, 171904/1 (2007).
[26]S. A. Medvedev, I. A. Trojan, M. I. Eremets, T. Palasyuk, T. M. Klapoetke, and J. Evers, J. Phys. Condens. Matter **21**, 195404/1 (2009).
[27]S. M. Peiris and T. P. Russell, J. Phys. Chem. A **107**, 944 (2003).
[28]U. Mueller, Z. Anorg. Allg. Chem. **392**, 159 (1972).
[29]H. K. Mao, P. M. Bell, J. W. Shaner, and D. J. Steinberg, J. Appl. Phys. **49**, 3276 (1978).
[30]H. K. Mao, J. Xu, and P. M. Bell, J. Geophys. Res. B **91**, 4673 (1986).
[31]A. P. Hammersley, S. O. Svensson, M. Hanfland, A. N. Fitch, and D. Hausermann, High Press. Res. **14**, 235 (1996).
[32]I. L. Spain and D. J. Dunstan, J. Phys. E: Sci. Instrum. **22**, 923 (1989).
[33]A. Boultif and D. Louer, J. Appl. Crystallogr. **37**, 724 (2004).
[34]T. Hahn, *International Tables for Crystallography*, Vol. A, 5th, revised edition (Space Group Symmetry, Kluwer Academic Publishers, Dordrecht, the Netherlands, 2001).
[35]J. Rodriguez-Carvajal, Physica B (Amsterdam) **192**, 55 (1993).
[36]W. Zhu, J. Xiao, and H. Xiao, J. Phys. Chem. B **110**, 9856 (2006).
[37]See Supplemental Material at http://link.aps.org/supplemental/10.1103/PhysRevB.84.064127 for unit cell parameters and volume per formula unit at varying pressures.
[38]F. Birch, Phys. Rev. **71**, 809 (1947).
[39]C. Ji, F. Zhang, D. Hou, H. Zhu, J. Wu, M.-C. Chyu, V. I. Levitas, and Y. Ma, J. Phys. Chem. Solids **72**, 736 (2011).